THE DESIGN, SYNTHESIS AND ANALYSIS OF HIGH-AFFINITY PEPTIDE-PEPTOID HYBRID LIGANDS THAT BIND EVH1 DOMAINS

&

THE SYNTHESIS OF 1-SUBSTITUTED *m*-TERPHENYLS THAT SERVE AS N^C^C AND O^C^C LIGANDS FOR USE IN CYCLOMETALLATED PLATINUM COMPLEXES

By

Eric J. Dimise

* * * * * * * * *

Submitted in partial fulfillment

of the requirements for

Honors in the Department of Chemistry

UNION COLLEGE

June, 2005

ABSTRACT

DIMISE, ERIC J. The design, synthesis and analysis of high-affinity peptide-peptoid hybrid ligands that bind EVH1 domains. Department of Chemistry, June 2005.

Protein-ligand interactions are often at the center of cellular regulatory processes. The Enabled/Vasodilator Stimulated Phosphoprotein Homology 1 (EVH1) domain of the Enabled/Vasodilator Stimulated Phosphoprotein (Ena/VASP) protein family has been linked to the regulation of the actin cytoskeleton through multiple protein-protein interactions via the recognition of polyproline amino acid sequences. Here, we examine the structural and physicochemical features of the EVH1 domain in an effort to design high affinity peptide-peptoid hybrid ligands that compete with EVH1's natural binding partners.

&

DIMISE, ERIC J. The synthesis of 1-substituted *m*-terphenyls that serve as N^C^C and O^C^C ligands for use in cyclometallated platinum complexes. Department of Chemistry, June 2005.

The unique photophysical properties of aryl, tridentate complexes of platinum have recently led to a surge in ligand design efforts. Here, we outline a facile synthetic route to platinum ligands with N^C^C and O^C^C binding modes, two classes of compounds that have yet to be investigated.

ACKNOWLEDGMENTS

First and foremost, I would like to thank Prof. Joanne D. Kehlbeck for providing such memorable and invaluable research opportunities. She was a conscientious, enthusiastic and caring advisor. She provided an undergraduate research experience that affirmed my goals for a future in academia. She is a model educator and will surely meet with much success in her future as a professor.

Next, I would like to thank Sarah-Jo Stimpson ('05) for her work on the EVH1 project. She has been (and will continue to be!) a lifelong friend and it was a pleasure to work with her. She endured many weeks of High Performance Liquid Chromatography with me, which is, at the very least, a profound comment about her character and her loyalty. I wish her much success as the future Dr. Sarah-Jo Stimpson, M.D.

I would like thank Adam Reeve ('07) for his work on the platinum ligand synthesis. He spent many hours (sometimes 24 hours straight) in the lab preparing starting materials. The project would not have progressed nearly as far without his hard work. It was a pleasure to work with him. In addition, I feel I can say without hesitation that between the two of us, the Kehlbeck Research Lab has the best collection of music in the department.

I would like to thank all of the Kehlbeck research students, both past and present, for their support and friendship. They are: James Miller ('05), Jim Bush ('05), and David E. Olson ('06).

I send my sincerest thanks to the other members of the chemistry department, both faculty and students, for being such wonderful people to work with. I will never forget my "Team Chem" family. Specifically, I would like to thank Prof. James Adrian

TABLE OF CONTENTS

III. **The synthesis of 1-substituted *m*-terphenyls that serve as N^C^C and O^C^C ligands for use in cyclometallated platinum complexes**

TABLE OF FIGURES

The design, synthesis and analysis of high-affinity peptide-peptoid hybrid ligands that bind EVH1 domains

Eric J. Dimise, Joanne D. Kehlbeck*
Department of Chemistry, Union College, Schenectady NY, 12308
June 2005

Abstract

Rationally designed, high affinity peptidomimetic molecules can be used to probe the interactions in protein-ligand systems. The Enabled/Vasodilator Stimulated Phosphoprotein Homology 1 (EVH1) domain's interactions with polyproline rich amino acid sequences in proteins such as Vinculin and Zyxin are well documented and suggest that EVH1 containing proteins play an intimate role in the regulation of actin cytoskeletal dynamics. Here, we aim to selectively interrupt the interactions of EVH1 with its natural ligands using high affinity peptide-peptoid hybrids that mimic the natural EVH1 binding partners. In doing so, we hope to gain a more thorough understanding of the specific interactions controlling the complex cytoskeletal machinery.

Protein-Ligand Interactions

Biochemical processes are often mediated by specific, moderate affinity protein-ligand interactions. Such interactions allow for site-specific, reversible molecular recognition events capable of evoking highly regulated biological responses. These interactions frequently occur among proteins, resulting in the formation of multi-protein systems capable of regulating complex cellular processes. Natural disruptions in these interactions (via mutation, improper protein folding, etc.) can result in disease states. On the contrary, non-natural disruptions imposed by rationally designed molecules are capable of shedding light on protein systems that are poorly understood or characterized. In addition, this method of investigation holds the potential for the discovery and development of novel medicinal and biotechnological agents.

The Enabled/Vasodilator Stimulated Phosphoprotein (Ena/VASP) protein family lies at the center of a complex protein recognition system linked to the regulation of the actin cytoskeleton. To elucidate the finer details of this system, a series of molecules have been designed to selectively disrupt the interactions between the well conserved Enabled/Vasodilator Stimulated Phosphoprotein Homology 1 (EVH1) domain, common to all Ena/VASP family members, and its natural binding partners. We hope to gain both functional and organizational knowledge of this protein system by monitoring the response these molecules produce in studies *in vivo* and by spectroscopically examining their binding properties *in vitro*. Ultimately, we aim to obtain a more thorough understanding of the nuances of protein-ligand interactions in complex multi-protein regulatory systems while concurrently developing new routes towards the discovery of novel therapeutic agents and biotechnological tools.

2

The Actin Cytoskeleton

Many biological processes that require cellular motility have been intimately linked with rearrangements of the actin cytoskeleton. These processes are diverse and encompass a broad range of cellular functions and cell types. For example, it has been found that actin based cell motility plays a key role in wound healing, axon elongation, cytokinesis, chemotaxis and cancer cell metastasis.(1-3) In addition, the bacteria *Lysteria monocytogenes* acquires its pathogenicity from its ability to hijack a host cell's actin assembly proteins, producing propulsive actin "comet tails" that allow it to move both intracellularly and intercellularly.(4) The current gap that exists between a thorough understanding of these processes and the structural and functional roles of the EVH1 domain can be bridged by employing rational molecular design.

The Enabled/Vasodilator Stimulated Phosphoprotein Homology 1 (EVH1) Domain

EVH1 is a highly conserved, non-catalytic protein domain present in all of the Ena/VASP family proteins including *Drosophila* Enabled (Ena), Mammalian Enabled (Mena), VASP, Ena-VASP- like protein (EVL) and Wiscott-Aldrich Syndrome Protein (WASP). They share a similar succession of conserved structural elements which include an N-terminal EVH1 domain, a central proline rich region and a C-terminal EVH2 domain.(5-7) Proteins that are known to regulate actin dynamics bind to each of these regions, forming intimate links between Ena/VASP family members and the actin cytoskeleton (Figure 1). The focal adhesion associated proteins Vinculin and Zyxin bind the EVH1 domain as does the surface protein ActA of *L. monocytogenes*.(4,8,9) It has been shown that the recently discovered protein, Palladin, also binds to the EVH1

3

domain.(2)   This is of particular interest because so little is known about the precise function of Palladin and because no structural information is available that can be used to elucidate functional information. The central proline rich region is known to bind the G-actin polymerizing Arp2/3 complex and the G-actin binding protein Profilin. The C-terminal EVH2 domain can bind F-actin and other EVH2 domains, allowing for the mass co-localization of the cytoskeletal regulatory machinery.(7)   Given the binding partners associated with each of the respective structural regions of the Ena/VASP proteins, the organizational/regulatory importance of this group of proteins to the dynamics of the actin cytoskeleton becomes clear.
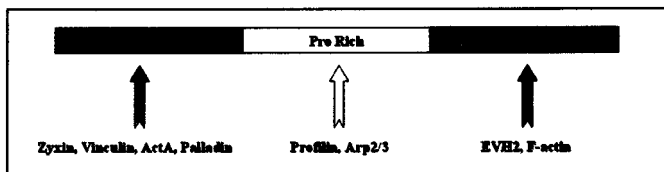
Figure 1. General domain structure of Ena/VASP family members and the proteins that bind to them.

The EVH1 domain has been structurally characterized.(10,11)   Containing approximately 112 amino acid residues, the bulk of the structure consists of a β sandwich formed by the stacking of two antiparallel β sheets comprised of a total of 7 β strands. Strand 7 is linked to a C-terminal α helix that runs parallel to the long axis of the β sandwich and connects the EVH1 domain to the other constituent structures of the Ena/VASP family. A cleft in the β structure forms the site of EVH1-ligand interaction. Ribbon structures highlighting important secondary structural elements are given in Figure 2.

4

Figure 2. (A) Succession of β strands in EVH1. (B) β strands 1, 5, 6 and 7 form one β sheet (green) and β strands 2, 3 and 4 form the other (yellow). [PDB accession: 1EVH]
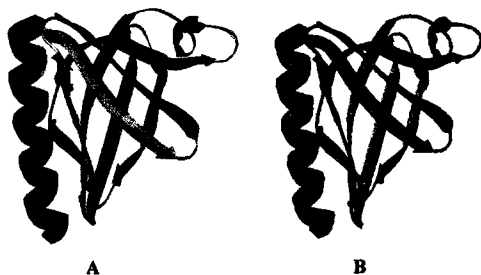
Polyproline Type II Helices

Central to EVH1-ligand binding is the EVH1 domain's ability to bind polyproline type II (PPII) helices. The PPII helix is a unique kind of secondary structure found in peptides rich in proline and is a vital structural component found in all of the EVH1 binding partners.(12) Figure 3 shows the PPII conformation of a typical EVH1 ligand.

Figure 3. The PPII helical conformation. (A) Four residue PPII helical segment viewed from the side. (B) Four residue PPII helical segment looking down the helical axis.

The PPII helix provides a unique chemical surface that lends itself well to moderate affinity binding interactions. The pyrrolidine ring formed by the cyclization of the proline side chain back upon the amide nitrogen provides a hydrophobic surface that compliments the side chains of the hydrophobic and aromatic amino acids and often results in weak peptide-protein surface interactions. PPII helices offer hydrogen bond accepting capabilities unique to polyproline peptides, both in number and geometry.

5

Unlike any other naturally occurring amino acid, proline does not have an amide hydrogen available to act as a hydrogen bond donor. In contrast, the backbone carbonyls are available to accept hydrogen bonds.(12)

The PPII structure also offers a unique conformational architecture that allows it to serve as a good ligand in specific molecular recognition events. These left handed helices have $\phi = -75°$ and $\psi = 145°$, with a helical repeat every three residues, a geometry exclusive to the PPII structure. Due to the rotational and conformational restrictions imposed by the cyclical side chain of proline, PPII helical sequences tend to suffer a smaller entropic loss when binding to a receptor. Finally, the shape of the PPII helix itself can serve as a discriminating factor in a binding pocket. It has long been known that the sequence PxxP is required for ligand binding to SH3 domains for example, which can only be satisfied by SH3 ligands that contain the PPII helical conformation. An examination of the binding pocket of EVH1 reveals that it also restricts its binding partners to those presenting the characteristics of the PPII helical conformation.(12)

The EVH1 Binding Groove

EVH1 binds its protein ligands in a deep and narrow V-shaped binding groove formed by strands $\beta1$, $\beta5$, $\beta6$ and $\beta7$. The groove contains the residues Tyr16, Trp23 and Phe77, which together form hydrophobic, aromatic grooves that selectively recognize protein ligands in the PPII helical conformation (Figure 4).(10,11) Peptide binding studies have shown that this groove binds ligands with the general sequence FPxϕP (where x is a variable residue and ϕ is a hydrophobic residue) and that also maintain the PPII conformation.(13) This observation serves to emphasize the importance of the PPII

6

conformation in EVH1-peptide *recognition*. (This should, of course, not serve to deemphasize or confuse the importance of electronics in determining the *affinity* between EVH1 and its ligands.) Regardless, due to the tight sterics of the binding groove, the vast majority of naturally occurring EVH1 peptide ligands have an FPPPP consensus sequence.

The phenylalanine residue N-terminal to the core PxɸP sequence is critical to EVH1-ligand binding.(10,11,13) Peptide binding studies demonstrate that sequences containing residues other than phenylalanine at this position lose most if not all of their EVH1 binding affinity. Structural studies indicate a binding pocket on EVH1 adjacent to the polyproline binding groove that is very specific to phenylalanine. When this phenylalanine residue is missing or altered, ligands lack the proper sterics for binding and thus exhibit a decrease in or complete loss of binding affinity.

Structural studies indicate that there are two hydrogen bonds that form between residues in the binding groove and the backbone carbonyls of proline 1 and proline 2 (the numbering system we employ is: $FP_1P_2P_3P_4$).(11) The Pro1 carbonyl accepts a hydrogen bond from Gln79, which is in close proximity to Phe77 and Tyr16. The Pro2 carbonyl accepts a hydrogen bond from the hydrogen on the indole nitrogen of Trp23. Both of these hydrogen bonds form as a result of the orientation of the backbone of the PPII helix relative to the binding groove.

Prehoda, Lee and Lim have solved the crystal structure of Mena EVHi with an FPPPP ligand bound to 1.8Å resolution. Figure 4 illustrates all of the characteristics of the EVH1 binding groove we have discussed thus far using this crystal structure.
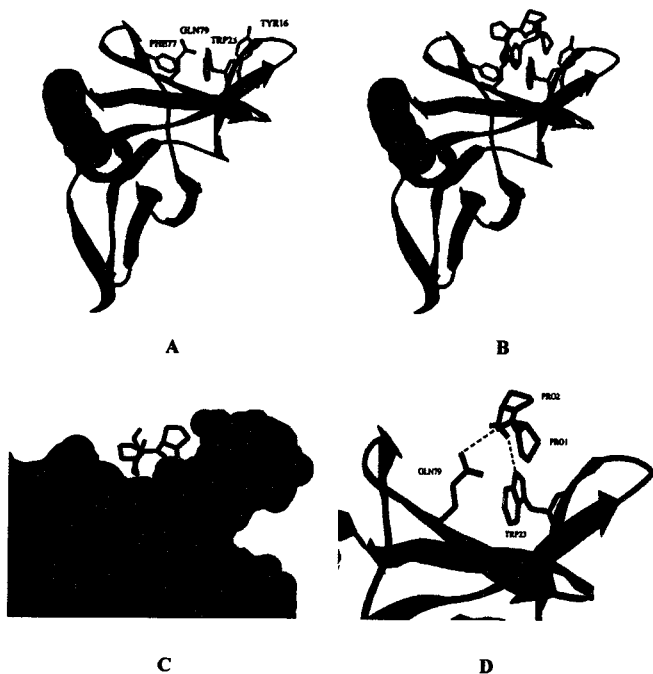
Figure 4. The binding groove of the EVH1 domain. **(A)** The three residues that make key hydrophobic contacts with the polyproline sequence of the ligand are Tyr16, Trp23 and Phe77. Gln79 is shown because it forms a hydrogen bond with Pro1. **(B)** EVH1 domain with FPPPP ligand bound. **(C)** Surface rendering of the EVH1 binding groove with ligand bound emphasizing the steric specificity of the Phe binding pocket. **(D)** Close up of the binding pocket showing the hydrogen bonds formed between the backbone carbonyls of Pro1 and Pro2 with Gln79 and Trp23, respectively.

Peptidomimetics and Rational Design: Peptoids

A major field in the study of protein-ligand interactions is peptidomimetics, where the goal is often to design and synthesize high affinity molecules that mimic and exhibit competitive binding with natural peptide ligands. Because reversibility of binding is often crucial to naturally occurring protein-ligand systems, most systems exhibit relatively modest binding affinities. Rationally designed, competitive, high affinity molecular mimics can thus serve as the tools to interrupt natural protein-ligand interactions and thus probe the structural/functional properties of protein-ligand systems of interest. This approach to the study of structure/function relationships among biomolecules is often less intrusive when used at the organismal level than the classical gene-knock-out approach. In the latter, the effects of the study are felt "globally" and are often permanent. Altering the genotype also often results in many unwanted or unexpected phenotypes. The peptidomimetic approach allows for the selective, modulated, nonpermanent interruption of interactions of interest. We propose to use the peptidomimetic approach to understand the EVH1-polyproline ligand system.

We are interested in a class of peptidomimetic foldamers (synthetic molecules that mimic biopolymers and *fold* into unique conformations in solution) called peptoids, a class of foldamers that are based on N-substituted glycine subunits.(14,15) These will serve as the foundation for our ligand design due to their many favorable physicochemical properties. The major structural difference between α-peptides and peptoids is the positioning of the R group on the peptoid amide nitrogen. This seemingly small structural change in the monomer subunit leads to several drastic differences in the properties of the polymer. The lack of an amide hydrogen eliminates the possibility of

9

hydrogen bonding between polymer backbones. This also results in a decrease in polarity of the backbone, giving peptoids greater membrane permeability than α-peptides. It has also been suggested that N-substitution provides peptoids with a heightened degree of protease resistance. Due to the lack of a chiral center in the peptoid subunit, peptoid monomers do not have any intrinsic handedness.(14) The general structures of peptides and peptoids are compared in Figure 5.
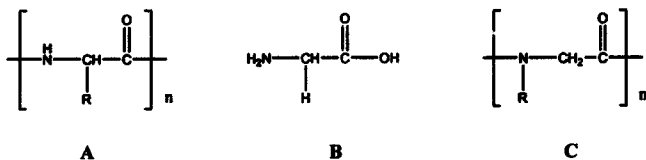

Figure 5. (A) General structure of an α-peptide. (B) The amino acid glycine. (C) General structure of a peptoid (an N-substituted glycine subunit).

Peptoids lend themselves nicely to the study of polyproline-binding protein systems, because, in addition to the advantages discussed above, peptoids are N-substituted like proline and aid in maintaining the PPII structure that is so crucial in systems such as EVH1. Initially, our molecular mimics will contain point substitutions of peptoids in the FPPPP binding sequence of EVH1. Thus, we will synthesize peptide-peptoid hybrids for our initial studies.

Merrifield sparked interest in solid phase peptide synthesis as early as the mid 1960's and was later awarded the Nobel Prize for his work in 1984. The solid phase methods are now very efficient and lend themselves nicely to the synthesis of long chain polypeptides.(16) We have chosen to prepare our hybrid molecules on an Fmoc (9-fluorenylmethoxycarbonyl) protected rink amide resin using Fmoc protected amino acids. Peptide synthesis is achieved via the repetition of a two step reaction sequence. In the first step, the Fmoc protecting group is removed from the resin (for the first amino acid) or from an exposed Fmoc protected amino acid using 20% piperidine. The newly exposed amine is then reacted with an Fmoc protected amino acid that has had its exposed carboxyl group converted to an activated ester with the coupling reagents 2-(1*H*-benzotriazol-1-yl)-1,1,3,3-tetramethyluronium hexafluorophosphate (HBTU) and N-hydroxybenzotriazole (HOBt). These steps are repeated for additional couplings. The steps are outlined in Figure 6, which shows the coupling of the first amino acid to the rink amide resin.
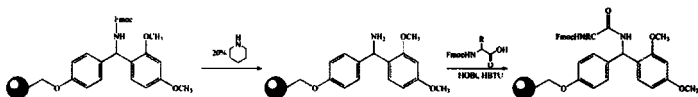

Figure 6. Two step Fmoc-amino acid coupling reaction on the solid phase.

With slight modification, peptoids tend to lend themselves quite nicely to the methods of solid phase peptide synthesis. Figure 7 outlines the process of inserting a peptoid residue into a growing peptide chain. Bromoacetic acid is treated with an activating reagent such as diisopropylcarbodiimide (DIC), converting its non-reactive

carboxyl to an activated ester. This reactive bromoacetic acid derivative is then added to the solid phase, where it undergoes an addition/elimination reaction with the free amine on the resin bead. In a second step, a primary amine replaces the bromine now attached to the free end of the solid phase via an S_N2 reaction, incorporating its nitrogen atom into the peptide backbone and providing the desired N-substituted functionality.
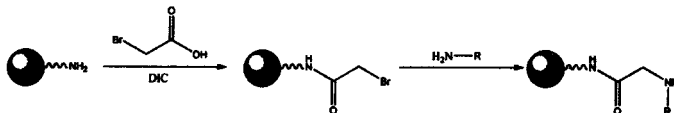

Figure 7. The two step addition of a peptoid residue on the solid phase.

The Rational Design of Palladin Mimics

In 2000, Parast and Otey identified a new protein that localized along actin stress fibers and focal adhesions and named it Palladin.(3,17) Later in 2004, they were able to show definitively that Palladin binds to the EVH1 domain of VASP using FPPPP and FPLPP sequences near its N-terminus.(2) Fluorescence microscopy studies showed clear co-localization of Palladin and VASP in regular patterns along stress fibers and at focal adhesions. Palladin is also known to bind to the actin cross linking protein α - actinin, suggesting that Palladin may serve both a localization and adapter function.(3) There is evidence to suggest that actin polymerization occurs at regular intervals along stress fibers, and it has been suggested that Palladin-Ena/VASP proteins may be instrumental in this process.(2) However, much work needs to be done before a definitive answer to any of these questions can be reached.

We propose to synthesize a series of peptide molecules that mimic the N-terminal EVH1 binding segment of Palladin containing the FPPPP consensus sequence. These

molecules will contain peptoid residues at key positions in the consensus sequence. Our aim is to design novel peptide-peptoid hybrids that will bind with higher affinity to EVH1 than the natural sequence present in Palladin. Affinity will be determined by performing fluorescence polarization binding studies on fluorescently labeled hybrid molecules and determining their dissociation constant (K_d) to EVH1. By interrupting the natural EVH1-Palladin interaction, we hope to gain insight into the function and localization of these binding partners in a reversible and selective manner.

When designing ligands that bind the EVH1 domain, the natural paradigm is the *L. monocytogenes* surface protein ActA. This has been shown to bind with the highest affinity (K_ds found on the order of 5μM).(11,13) An ActA binding sequence is DFPPPPTDEEL. Given in bold is the obligatory Phe residue N-terminal to the central PPPP sequence. Also of great interest in this sequence is the succession of acid residues C-terminal to the binding sequence. The crystal structure suggests that these acid residues, negative at physiological pH, can form salt bridges with protonated basic residues on the surface of EVH1.(11) Binding studies show that affinity increases with increasing acidic residues C-terminal to the central consensus sequence.(11) The segment of Palladin containing the EVH1 binding sequence is PSPPFPPPPPAFPEL. Thus, the glutamic acid residue C-terminal to the consensus should be retained in any proposed molecular mimic.

Using ActA as a guide, we were free to investigate all possible peptoid substitutions in the consensus sequence. We considered the general binding requirements of the EVH1 domain embodied in the "formula" FPxϕP. Peptide binding studies have shown that replacement of the Pro 1, Pro 4 and Phe residues is detrimental to ligand

binding affinity.(11,13) However, positions 2 and 3 are more readily substituted with other amino acids. Therefore, we will attempt to replace these residues with peptoids that can take a more active role in ligand binding and increase the overall affinity of the ligand for the EVH1 domain.

In the interest of building the minimal number of molecules, rational design methods using computer models were employed to develop two series of Palladin mimics. The first series of Palladin mimics were designed to replace Pro3. Crystal structure analysis of the EVH1 binding groove shows Pro3 positioned in an aromatic, hydrophobic pocket formed by Phe77 and Trp23. The plane of the pyrrolidine ring of Pro3 lies parallel to the plane of the phenyl ring of Phe77 with a separation of approximately 4Å between the two rings. In addition, the rings are slightly offset, such that the edge of the Pro ring seems to abut the edge of the Phe ring when viewed from above. Given the positioning of the Pro, Phe and Trp residues in this section of the binding groove, it is reasonable to suggest that Van der Waals forces constitute the prominent stabilizing binding interactions. Figure 8 highlights these details.
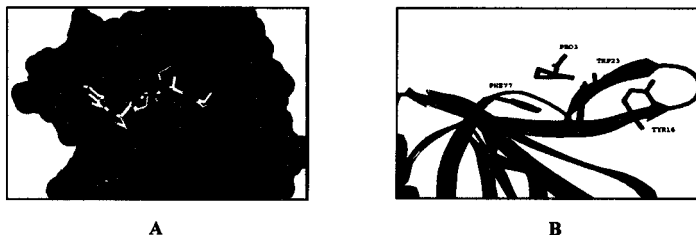

| A | B |

Figure 8. Computer modeling studies of the binding of Pro3 to the EVH1 domain. (A) EVH1 surface representation with ligand bound. Pro3 is indicated. The plane of the ring of Pro3 lies parallel to the surface of the EVH1 binding groove. (B) Ribbon structure of the EVH1 binding groove with binding groove residues and Pro3 shown. Pro3 sits in an aromatic pocket between Phe77 and Trp23. The plane of the Pro ring lies parallel to the face of the Phe77 ring, but is slightly offset.

The series 1 Palladin mimics will allow us to explore the electronic properties and steric limits of the pocket formed by Phe77 and Trp23 by replacing Pro3 with N-substituted groups containing five and six membered aromatic rings. By introducing aromatic groups in place of the aliphatic side chain of proline, we explore the possibilities of introducing $\pi-\pi$ interactions between the aromatic residues of the EVH1 binding groove and the ligand. We will explore the sterics of the binding pocket by incorporating a series of methylene spacers between the backbone nitrogen and the aromatic rings. Doing so will allow us to examine the effects of increasing the freedom of motion of the aromatic rings. The methylene spacers may allow the rings to "find" a sterically favorable position in the binding pocket. We will also be able to determine the spacer length that provides the optimum amount of $\pi-\pi$ overlap between the aromatic groups of the ligand and the binding pocket. The effects of increasing the steric bulk of the peptoid side chain with the addition of subsequent methylene spacers will also be explored. By introducing rings of different size, we can examine which size is most favorable for this particular environment. A thiophene functionality has been chosen for the five membered aromatic group due to the instability of a cyclopentadienyl substituent. It is not uncommon for sulfur to be used as a methylene isostere and the incorporation of sulfur reduces the likelihood of new hydrogen bond formation, which we want to avoid due to our specific interest in the examination of hydrophobic and aromatic interactions. These peptoid groups will be introduced as primary amines via the synthetic scheme outlined in Figure 7. The structures of the primary amines to be used in the synthesis are given in Figure 9A. Figure 9B is an illustration of the rational design concepts outlined above in the series 1 proposal using the benzene peptoid substituent as an example.
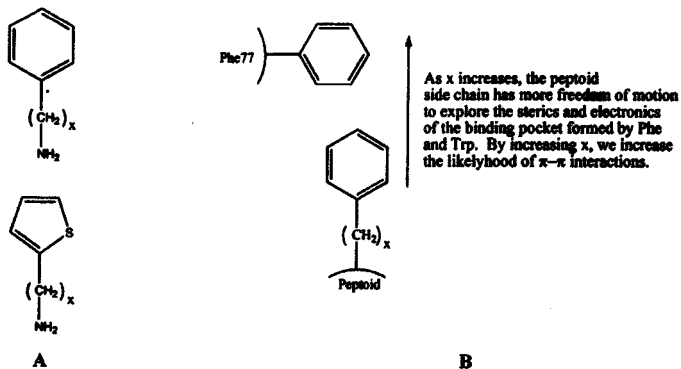
As x increases, the peptoid side chain has more freedom of motion to explore the sterics and electronics of the binding pocket formed by Phe and Trp. By increasing x, we increase the likelyhood of $\pi-\pi$ interactions.

A   **B**

Figure 9. (A) Series 1 Pro3 peptoid side chain substituents. All amino nitrogens will be incorporated into the peptide backbone via the synthetic scheme outlined in Figure 7. (B) This series investigates the affects of aromaticity, ring size and methylene linker number on binding. [x = 0,1,2]

In the second series of Palladin mimics, we seek to replace Pro2 of the EVH1 consensus sequence. The side chain of Pro2 is dissimilar to the other Pro residues in the consensus sequence in that it does not make any close contacts with the important binding groove residues. Instead, it is positioned above the binding groove, serving mostly to bridge Pro1 and Pro3 and to help maintain the PPII conformation. The directionality of the N-R bond of Pro2 is of interest. This bond points in the direction of the Tyr16 hydroxyl substituent and has an offset of about 14° at a distance of 5.2Å. Figure 10 shows the orientation of Pro2 in the EVH1 binding groove.
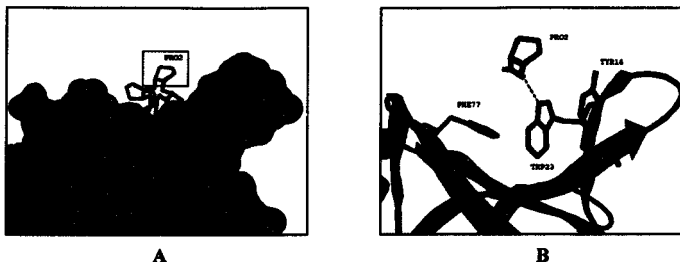
Figure 10. Computer modeling studies of the binding of Pro2 to the EVH1 domain. **(A)** Surface rendering of EVH1 shows that Pro2 sits above the binding groove bridging Pro1 and Pro3. **(B)** The ribbon structure of EVH1 shows the important binding groove residues and Pro2. The directionallity of the side chain bond of the Pro2 backbone nitrogen towards the hydroxyl of Tyr16 is clear.

Reconsidering the general consensus sequence "formula" FPxϕP, we see that we have maximum flexibility in substituting Pro2. Due to the orientation of the backbone-side chain N-R bond towards the Tyr16 hydroxyl, we plan to introduce a series of hydrogen bond donor/acceptor peptoid residues. In introducing a primary amine, we provide two hydrogen atoms capable of acting as hydrogen bond donors to the Tyr hydroxyl. In addition, we introduce the additional electron pair on the nitrogen, capable of accepting a hydrogen bond from the Tyr hydroxyl. Should we introduce a primary alcohol side chain, then we reduce our hydrogen bond donating capability by one atom relative to a primary amine, but we increase our hydrogen bond accepting capability by one electron pair. As in Series 1, a succession of methylene spacers will be incorporated between the backbone nitrogen and the hydrogen bond donor/acceptor groups to see which length can best span the gap between the ligand and the Tyr residue. The structures of the Series 2 primary amines to be incorporated as peptoids are given in

17

Figure 11A. Figure 11B is an illustration of the rational design concepts outlined in the series 2 proposal above.
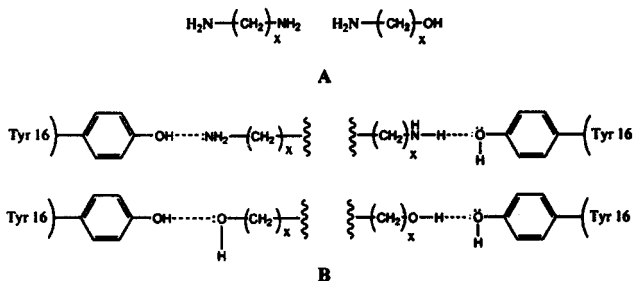

A

B

Figure 11. (A) Series 2 Pro 2 peptoid side chains. (B) Primary amines and alcohols will be used to determine which group is best suited for forming ligand-Tyr16 hydrogen bonds. These will be incorporated into the peptide via the reaction scheme outlined in Figure 7. [x = 0,1,2]

Fluorescence Polarization Binding Studies

To compare the binding affinities of our peptide-peptoid hybrid molecules to the naturally occurring EVH1 binding partners, we will determine the dissociation constant (K_d) of the EVH1-hybrid complexes using fluorescence polarization.(18,19) In general, for a ligand (L) and a receptor (R), the following equilibrium can be written:
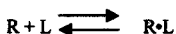
$$R + L \rightleftharpoons R \cdot L$$

where R•L is the receptor-ligand complex. The equilibrium constant is given by:

[Eq. 1]
$$K_a = \frac{[R \cdot L]}{[R][L]}$$

and is referred to as the association constant, denoted K_a. The dissociation constant is the equilibrium constant for the reverse reaction and is the inverse of the K_a:

[Eq. 2]
$$K_d = \frac{1}{K_a} = \frac{[R][L]}{[R \cdot L]}$$

18

A binding curve can be fit to fluorescence polarization data using the following equation

(Eq. 3) and curve fitting software.(19)

$$P([R]) = P_{min} + (P_{max} - P_{min}) \left[\frac{K_a[L] + K_a[R] + 1 - \sqrt{(K_a[L] + K_a[R] + 1)^2 - 4K_a[L][R]}}{2K_a[L]} \right]$$

P([R]) = polarization as a function of receptor concentration
P_{min} = polarization of free ligand
P_{max} = polarization of sample with highest receptor concentration
K_a = association constant
[L] = fluorescent ligand concentration
[R] = receptor concentration

Given the value of K_a determined from the fit of Eq. 3, the simple relationship given in

Eq. 2 can be applied to obtain K_d. A sample binding curve is given in Figure 12.
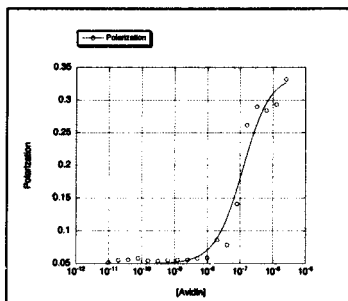

Figure 12. Binding curve produced by biotin-avidin complexation. Polarization is plotted against avidin concentration. The binding curve was fit using the computer graphing utility KaleidaGraph and Eq. 3. The avidin-biotin system was used as a tool for fluorescence polarization method development.

In order to conduct fluorescence polarization studies, a fluorophore must be coupled to the peptide-peptoid hybrid ligands. This can be achieved via a simple reaction between the deprotected N-terminus of the ligand on the solid phase and a reactive fluorophore. There are a wealth of fluorophores that are available commercially that lend themselves well to this type of reaction. Figure 13 outlines the coupling reaction between

19

References

1. Malika Boukhelifa, M. M. P., Juli G. Valtschanoff, Anthony S. LaMantia, Rick B. Meeker, and Carol A. Otey. (2001) *Molecular Biology of the Cell* 12, 2721-2729

2. Malika Boukhelifa, M. M. P., James E. Bear, Frank B. Gertler, and Carol A. Otey. (2004) *Cell Motility and the Cytoskeleton* 58, 17-29

3. Otey, M. M. P. a. C. A. (2000) *The Journal of Cell Biology* 150(3), 643-655

4. Kirsten Niebuhr, F. E., Ronald Frank, Matthias Reinhard, Eugen Domann, Uwe D. Carl, Ulrich Walter, Frank B. Gertler, Jurgen Wehland and Trinad Chakraborty. (1997) *The EMBO Journal* 16(17), 5433-5444

5. Adam V. Kwiatkowski, F. B. G. a. J. J. L. (2003) *Trends in Cell Biology* 13(27), 386-392

6. Linda J. Ball, T. J., Hartmut Oschkinat, Ulrich Walter. (2002) *FEBS Letters* 513, 45-52

7. Matthias Krause, J. E. B., Joseph J. Loureiro and Frank B. Gertler. (2002) *Journal of Cell Sciences* 115, 4721-4726

8. Beth Drees, E. F., Julie Fradelizi, Daniel Louvard, Mary C. Beckerle, and Roy M. Golsteyn. (2000) *The Journal of Biological Chemistry* 275(29), 22503-22511

9. Klemens Rottner, M. K., Mario Gimona, J. Victor Small, and Jurgen Wehland. (2001) *Molecular Biology of the Cell* 12, 3103-3113

10. Alexander A. Fedorov, E. F., Frank Gertler, Steven C. Almo. (1999) *Nature Structural Biology* 6(7), 661-665

11. Kenneth E. Prehoda, D. J. L., and Wendell A. Lim. (1999) *Cell* 97, 471-480

12. Creamer, B. J. S. a. T. P. (1999) *Protein Science* 8, 587-595

13. Jurgen Zimmermann, R. K., Rudolf Volkmer-Enger, Thomas Jarchau, Ulrich Walter, Hartmut Oschkinat, and Linda J. Ball. (2003) *The Journal of Biological Chemistry* 278(38), 36810-36818

14. Kent Kirshenbaum, A. E. B., Richard A. Goldsmith, Philippe Armand, Erin K. Bradley, Kiet T.V. Truong, Ken A. Dill, Fred E. Cohen, and Ronald N. Zuckermann. (1998) *Proc. Natl. Acad. Sci.* 95, 4303-4308

15. Philippe Armand, K. K., Richard A. Goldsmith, Shauna Farr-Jones, Annelise E. Barron, Kiet T.V. Truong, Ken A. Dill, Dale F. Mierke, Fred E. Cohen, Ronald N. Zuckermann, and Erin K. Bradley. (1998) *Proc. Natl. Acad. Sci.* 95, 4309-4314

16. White, W. C. C. a. P. D. (2000) *Fmoc Solid Phase Peptide Synthesis: A Practical Approach*, Oxford University Press, Oxford

17. Olli-Matti Mykkanen, M. G., Mikko Ronty, Maciej Lalowski, Paula Salmikangas, Heli Suila, and Olli Carpen. (2001) *Molecular Biology of the Cell* 12, 3060-3073

18. Krull, T. L. M. a. U. J. (2003) *Analyst* 128, 313-317

19. Lee, T. H. a. J. C. (1990) *Proc. Natl. Acad. Sci.* 87, 1744-1748

20. (2002/2003) *Molecula Probes Handbook of Fluorescent Probes and Research Products*, 9 Ed.

The synthesis of 1-substituted *m*-terphenyls that serve as N^C^C and O^C^C ligands for use in cyclometallated platinum complexes

Eric J. Dimise, Joanne D. Kehlbeck*
*Department of Chemistry, Union College, Schenectady NY, 12308*
*June 2005*

Abstract

Aryl, tridentate ligands capable of forming complexes with platinum are of interest due to their unique luminescent properties. Possible applications range from chemical sensing and solar energy storage and conversion to their use in organic light emitting diodes (OLEDS). Ligands that have N^C^C and O^C^C binding modes have yet to be investigated. Here, we outline an expeditious synthetic route to this new class of compounds. The ability of these ligands to bind platinum with the desired binding mode is an inherent property of the ligand architecture and is reflected in the stepwise addition of the N, C, C or O, C, C moieties in the synthesis.

Introduction

Interest in the luminescent properties of complexes of platinum with aryl, tridentate ligands has recently led to a wealth of ligand design strategies aimed at optimizing fluorescence excited state lifetimes and quantum yields in this relatively new class of compounds.[1-6] The ability to fine tune these properties could lead to multiple applications in chemical sensing and solar energy storage and conversion. In addition, such complexes are candidates for incorporation into organic light emitting diodes (OLEDS). To date, the luminescent properties of ligands with N^C^N, C^N^C, C^N^N and N^N^N binding modes have been investigated.


X = C, N
R = electron donating/withdrawing
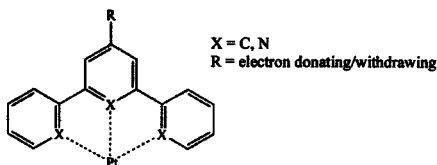
These studies have shown that excited state lifetimes and quantum yields can indeed be modulated by controlling the binding mode of the ligand and by substituting electron withdrawing and donating groups on the non-metallating parts of the ligand.[4,6] Here, we propose a facile synthetic route to a new class of aryl, tridentate platinum ligands with N^C^C and O^C^C binding modes based on a 1-substituted *m*-terphenyl structure.

X = N, O
R = H, aryl, alkyl

23
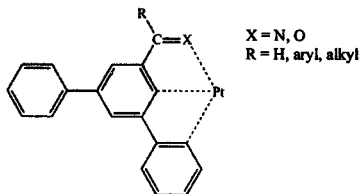
The metallation process puts specific demands on the ligand architecture to ensure that N^C^C and O^C^C binding is achieved. Metallation is initiated via coordination of the platinum center to the nitrogen or oxygen atom. The carbon-metal bonds are then formed through an oxidative addition/reductive elimination mechanism.[7,8] Due to the placement of the nitrogen and oxygen atoms in N^C^C and O^C^C ligands, a simple biphenyl structure would yield the bidentate, kinetic product instead of the desired tridentate product.
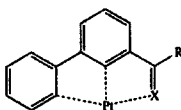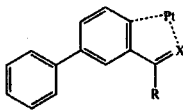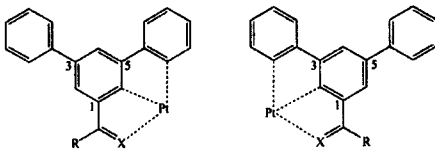

**Desired Tridentate Product**   **Bidentate Kinetic Product**

To circumvent this problem, we have designed a series of ligands based on a 1-substituted *m*-terphenyl structure. This design ensures that metallation occurs in an N^C^C or O^C^C fashion regardless of the position of the nitrogen or oxygen atom during the N-Pt or O-Pt complexation step of the metallation process.

Ligand synthesis can be viewed as a three step process in which (1) the "central" ring of the *m*-terphenyl is functionalized properly for further coupling reactions at the 1, 3 and 5 positions, (2) the two "peripheral" rings are added to positions 3 and 5 of the "central" ring and (3) the position 1 functionality is added to afford the desired product

24

(Scheme I). This synthetic scheme can be realized using 2,4,6-tribromoaniline as the starting material. Simple Sandmeyer chemistry can be employed in step 1 to convert 2,4,6-tribromoaniline to 2,4,6-tribromoiodobenzene (1). When treated with phenylmagnesium bromide, 1 readily forms reactive benzyne species that afford 1-bromo-3,5-diphenylbenzene (2) as was outlined by Hart.[9] The brominated 1 position of the *m*-terphenyl is left available for conversion to Grignard 3 which can then be used in a variety of reactions to afford the desired products (4).
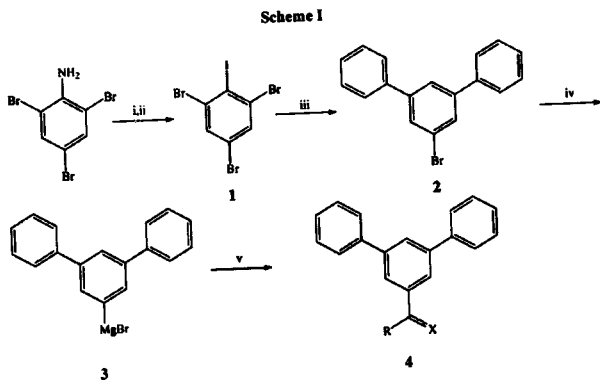
Scheme I

(i) NaNO$_2$, conc. HCl, 0 °C, 30 min (ii) KI, rt, 1 h (iii) PhMgBr, reflux, 1 h; rt, 12 h (iv) Mg turnings, THF, reflux, 1 h (v) various reagents

Results and Discussion

The coupling of PhMgBr to 1 to afford 2 is central to Scheme I in that it provides the *m*-terphenyl structure that is critical to the N^C^C and O^C^C binding mode and at the same time leaves the 1 position available for further chemistry. 2,4,6-tribromoaniline is an ideal starting material because it provides a facile route to 2, can be used in large

quantities and provides acceptable yields.[9] Grignard **3** is readily prepared in refluxing THF with a slight excess of magnesium. With **3** in hand, a series of reactions were employed to give formyl (**5**), acetyl (**6**) and pyridyl (**7**) substituted products at the 1 position.

5 R = H
6 R = CH₃

7
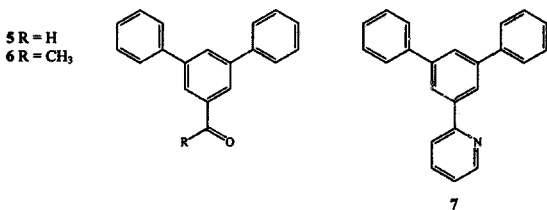
Olah has outlined a series of formylation reactions using N-formylmorpholine as a formylating agent.[10] We employed this chemistry in, what is to date, the most expeditious route to compound **5**. Prior synthesis of **5** employed a lithium aluminum hydride reduction of the carboxylic acid, which gave only modest yields. The formylation outlined here gives **5** in one step from **3** in good yield (73%).
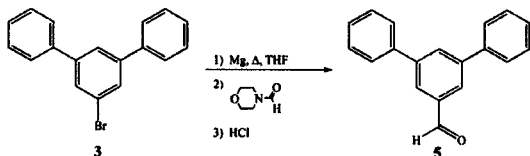

The 1-acetylated *m*-terphenyl **6** was prepared by the reaction of **3** with acetic anhydride. This reaction gives modest yields (51%) but provides a quick and easy route to **6**.
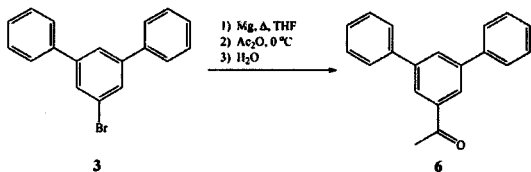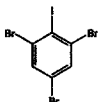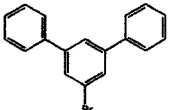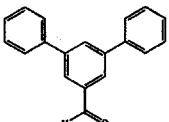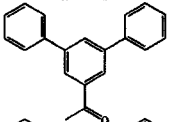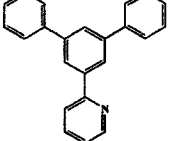
Special care had to be taken to avoid a second addition of **3** to the desired acetylated product. We employed an inverse addition technique outlined by Leazer whereby **3** was slowly added to a large excess of acetic anhydride.[11] When these measures are taken, the bi-substituted product expected from the direct addition of acetic anhydride to **3** is not produced.

The m-terphenylpyridine (**7**) was prepared by a Kumada-like Ni catalyzed coupling reaction. Herrmann recently reported on the success of several high yield coupling reactions of halogenated aromatic heterocycles to aryl Grignards using imidizolium ligands in the presence of Ni(acac)$_2$.[12] Here, **3** is coupled to 2-chloropyridine in the presence of Ni(acac)$_2$ and 1,3-bis-(2,4,6-trimethylphenyl)imidizolium to afford **7**.

3   **7**
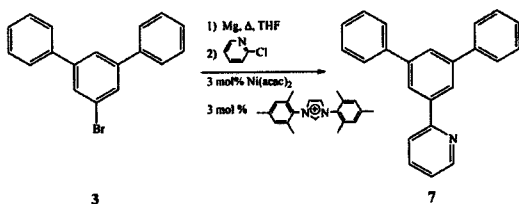
GC-MS analysis of the initial attempt of the preparation of **7** indicates two chromatographic peaks of the correct mass. This suggests the formation of isomers during the catalytic cycle. Future work will aim to correct this as the combined yield is relatively high (82%).

Table I. Products and Reaction Conditions of Compounds in Scheme I

Entry	Product	Conditions	Yield (%)
1		0 °C, 30 min : rt, 1h	58
2		reflux, 1 h : rt, 12 h	63
3		reflux, 1 h : rt, 30 min	73
4		reflux, 1 h : 0 °C, 2 h	51
5		reflux, 1 h : rt, 18 h	82

Experimental Section

General Procedures. ^{1}H NMR and ^{13}C NMR spectra were obtained using a Varian Gemini 2020 200MHz spectrometer with CDCl$_3$ solvent using Si(CH$_3$)$_4$ as an internal standard. Chemical shifts are reported in δ units (ppm). GC-MS analysis was performed on an Agilent 6890N gas chromatograph equipped with an N10149 autosampler coupled to an Agilent 5973 mass spectrometer. Anhydrous magnesium sulfate was used as the drying reagent in all reactions. All reactions were run under an atmosphere of dry nitrogen except in the preparation of (**1**) 2,4,6-tribromoiodobenzene. All reagents and solvents were purchased from Sigma-Aldrich and were used without additional purification.

    (**1**)   **2,4,6-tribromoiodobenzene.** A solution of sodium nitrite (3.28 g, 47.5 mmol) in 15 mL of water was added dropwise to a mechanically stirred slurry of 2,4,6-tribromoaniline (15 g, 45.5 mmol) in 23 mL of concentrated HCl at 0 °C. Stirring was continued for 30 min after complete addition of sodium nitrite. The diazonium salt was slowly transferred through a glass wool filter to a solution of potassium iodide (75.53 g, 0.455 mol) in 114 mL of water. The solution was stirred vigorously with both magnetic and mechanical stirring for 1 h at room temperature. 200 mL of CH$_2$Cl$_2$ and 20 mL of 0.5 M Na$_2$SO$_3$ were added successively. The aqueous layer was separated and washed with CH$_2$Cl$_2$. The combined organic layers were washed with 10% NaOH and saturated NaCl and dried. A red solid was isolated upon solvent removal. Recrystalization in 25% hexane/CH$_2$Cl$_2$ gave 11.6 g (26 mmol) of pure product (58%), mp 101-103 °C. ^{1}H NMR δ 7.71 (s, 2H). TLC (10% CH$_2$Cl$_2$/hexane) R$_f$ 0.61.

(2)   **1-bromo-3,5-diphenylbenzene.** A solution of **1** (10.0 g, 22.7 mmol) in 200 mL dry THF was added dropwise over 1 h to a 227 mL stirred, refluxing solution of 1 M phenylmagnesium bromide in THF (Sigma-Aldrich). Reflux was continued for 1 h after complete addition of **1**. Stirring was continued for 12 h at room temperature. Excess phenylmagnesium bromide was quenched with saturated NH_4Cl. The aqueous layer was washed with diethyl ether.   The combined organic layers were washed with saturated NaCl and dried.   A white solid was isolated after solvent removal. Recrystalization in 40% CH_2Cl_2/hexane gave 4.4 g (14.3 mmol) of pure product (63%), mp 102-104 °C. TLC (30% CH_2Cl_2/hexane) R_f 0.57.

(5)   **3,5-diphenylbenzaldehyde.** A solution of **2** (3.09 g, 10 mmol) in 10 mL dry THF was added dropwise to a stirred, refluxing mixture of magnesium turnings (0.27 g, 11 mmol) in 10 mL dry THF. A crystal of iodine was added to aid in Grignard initiation. Reflux was continued for 1 h after complete addition of **2**. A solution of *N*-formylmorpholine (10 mmol) in 10 mL dry THF was slowly transferred via canula to the stirring *m*-terphenyl Grignard and was stirred at room temperature for 30 min. Excess Grignard was quenched with 3 M HCl to a pH of 2. The aqueous layer was washed with diethyl ether and the combined organic layers were washed with saturated $NaHCO_3$ and NaCl. The product was purified by flash chromatography (30% CH_2Cl_2/hexane, 200-425 mesh silica gel) and recrystalized in 30% CH_2Cl_2/hexane to give 1.37 g (5.29 mmol) of pure product (53%). TLC (30% CH_2Cl_2/hexane) R_f 0.14.

(6)   **3,5-diphenylacetophenone.** A solution of **2** (0.500 g, 1.62 mmol) in 8 mL dry THF was added dropwise to a stirred, refluxing mixture of magnesium turnings (0.064 g, 2.62 mmol) in 8 mL dry THF. A crystal of iodine was added to aid in Grignard

initiation. Reflux was continued for 1 h after complete addition of **2**. The *m*-terphenyl Grignard was then slowly transferred via canula to a stirring solution of acetic anhydride (5 mL 99.5%, 52.9 mmol) at 0 °C. After 2 h of stirring at 0 °C, the reaction was quenched with water. The aqueous layer was washed with diethyl ether and the combined organic layers were washed with 10% NaOH and saturated NaCl and dried (51% by GC-MS).

(7) **m-terphenylpyridine.** A solution of **2** (0.77 g, 2.5 mmol) in 2.5 mL dry THF was added dropwise to a stirred, refluxing mixture of magnesium turnings (0.0851 g, 3.5 mmol) in 2.5 mL dry THF. A crystal of iodine was added to aid in Grignard initiation. Reflux was continued for 1 h after complete addition of **2**. The *m*-terphenyl Grignard was added dropwise by canula transfer to a stirred solution of 1.7 mmol 2-chloropyridine, 0.051 mmol (3 mol%) Ni(acac)$_2$, and 0.051 mmol (3 mol%) 1,3-bis-(2,4,6-trimethylphenyl)imidizolium in 1.7 mL dry THF at room temperature and was allowed to stir for 18 h. The reaction was quenched with methanol. The methanol layer was washed with diethyl ether and the combined organic layers were washed with saturated NaCl and dried. GC-MS analysis indicates two peaks matching the product mass with a combined peak percentage of 82% based on the disappearance of **3**.

References

(1)   Andreas Hofmann, L. D., and Rudi van Eldik *Inorg. Chem.* **2003**, *42*, 6528-6538.

(2)   Charles B. Blanton, Z. M., Randy J. Shaver, and D. Paul Rillema *Inorg. Chem.* **1992**, *31*, 3230-3235.

(3)   Hershel Jude, J. A. K. B., and William B. Connick *Inorg. Chem.* **2002**, *41*, 2275-2281.

(4)   J.A. Gareth Williams, A. B., E. Stephen Davies, Julia A. Weinstein, and Claire Wilson *Inorg. Chem.* **2003**, *42*, 8609-8611.

(5)   Matthew Polson, S. F., Valerio Bertolasi, Marcella Ravaglia, and Franco Scandola *Inorg. Chem.* **2004**, *43*, 1950-1956.

(6)   Qing-Zheng Yang, L.-Z. W., Zi-Xin Wu, Li-Ping Zhang, and Chen-Ho Tung *Inorg. Chem.* **2002**, *41*, 5653-5655.

(7)   Crabtree, R. H. *The Organometallic Chemistry of the Tranistion Metals*; 2nd ed.; John Wiley & Sons, Inc.: New York, 1994.

(8)   Tilset, M. L. a. M. *Chemical Reviews* **2004**.

(9)   Chi-Jen Frank Du, H. H., and Kwok-Keung Daniel Ng *J. Org. Chem.* **1986**, *51*, 3162-3165.

(10)   George A. Olah, L. O., and Massoud Arvanaghi *J. Org. Chem.* **1984**, *49*, 3856-3857.

(11)   Johnie L. Leazer, J., Raymond Cvetovich, Fuh-Rong Tsay, Ulf Dolling, Thomas Vickery, and Donald Bachert *J. Org. Chem.* **2003**, *68*, 3695-3698.

(12)   Volker P.W. Bohm, T. W., Christian W.K. Gstottmayr, and Wolfgang A. Herrmann *Angew. Chem. Int. Ed.* **2000**, *39*, 1602-1604.